

A synthetic urinary probe-coated nanoparticles sensitive to fibroblast activation protein α for solid tumor diagnosis

Xinwei Feng^{1,*}Qifan Wang^{1,*}Yuehua Liao¹Xie Zhou²Yidan Wang³Wanli Liu⁴Ge Zhang¹

¹Department of Microbial and Biochemical Pharmacy, School of Pharmaceutical Sciences, Sun Yat-sen University, Guangzhou, ²Department of Medical Chemistry, School of Pharmaceutical Sciences, Sun Yat-sen University, Guangzhou, ³Department of Biotechnology, School of Life Science, Sun Yat-sen University, Guangzhou, ⁴Department of Clinical Laboratory Medicine, Sun Yat-sen University Cancer Center, Guangzhou, China

*These authors contributed equally to this work

Abstract: We developed fibroblast activation protein α (FAP α)-sensitive magnetic iron oxide nanoparticles (MNPs) by conjugating a substrate-reporter tandem peptide as a synthetic biomarker to the surface of MNPs (marker-MNPs). In vitro, the marker-MNPs showed stability when treated with serum or urine and exhibited high susceptibility and specificity for FAP α enzyme and 3T3/FAP α cell line. Furthermore, the marker-MNPs were administered to esophageal squamous cell carcinoma xenograft tumor mice; they reached the tumor tissues in the mice, where they were cleaved effectively by the local overexpressed FAP α to release the reporter peptide and filter it into the urine. The tumor targeting and biodistribution of marker-MNPs were verified by in vivo imaging. The cleaved reporter peptides in urine detected by enzyme-linked immunosorbent assay have high diagnostic accuracy for esophageal squamous cell carcinoma (area under the receiver-operating characteristic curve = 1.0). Our study implies a promising strategy of utilizing the low-cost and noninvasive synthetic urinary probe-coated nanoparticles for the diagnosis of FAP α -positive solid tumors, except for in renal cancer.

Keywords: synthetic urinary probe, magnetic iron oxide nanoparticles, fibroblast activation protein α , tumor diagnosis

Introduction

Nanotechnology-based approaches bring new hope to the arena of cancer detection. Nanomaterial-based diagnostics, which is combined with the design of highly sensitive probes for cancer detection, has tremendous potential to improve the clinical paradigms of cancer diagnosis.¹ Currently, magnetic iron oxide nanoparticles (MNPs) have raised much interest due to emerging applications for noninvasive imaging and therapy.²

Tumor biomarkers are used to help detect some types of cancer, but they are usually rare, especially at early tumor stage, and not enough to diagnose cancer alone. The development of synthetic biomarkers, which are substrate peptides of some disease-associated enzymes, may broaden the applicability of biomarkers such as using urinary monitoring.^{3,4} The synthetic biomarkers conjugated to nanoparticles probe reach the disease sites in vivo. Next, in response to cleavage by local dysregulated proteases, they can release synthetic reporters that then filter into urine for mass spectrometer or enzyme-linked immunosorbent assay (ELISA) analysis.⁵ These approaches have been studied in detecting cancer and thrombosis and have shown high sensitivity and specificity as a simple and noninvasive method.⁶

Tumor microenvironment plays many critical roles in the tumor development. Cancer-associated fibroblasts (CAFs), with a key characteristic of expression of

Correspondence: Ge Zhang
School of Pharmaceutical Sciences,
Sun Yat-sen University, No 132
Waihuan Road East, University Town,
Guangzhou 510006, China
Tel/fax +86 20 3994 3021
Email zhangge@mail.sysu.edu.cn

fibroblast activation protein α (FAP α /Seprase), actively interact with tumor cells to promote cancer growth and support malignancy.⁷ FAP α is transmembrane serine protease that cleaves propyl peptide (Pro-Xaa) bonds of extracellular matrix in the microenvironment of most solid tumors.⁸ In addition, FAP α is selectively expressed in the stromal fibroblasts associated with epithelial cancers, whereas it has low or undetectable expression in the resting fibroblasts of normal adult tissues. Importantly, FAP α was found to show overexpression in numerous types of cancer tissues,⁹ whereas circulating FAP α levels were extremely low in most types of cancer.^{10–12} Multiple studies demonstrated that FAP α has the potential to be a promising target for designing tumor-targeted drugs and imaging agents.^{13,14}

In this study, we developed FAP α -sensitive MNPs by conjugating a substrate-reporter tandem peptide as a synthetic biomarker to the surface of MNPs (marker-MNPs) via a facile one-pot synthesis method. Dextran and polyethylene glycol (PEG)-coated MNPs were used to reduce the cytotoxicity and increase the stability and circulation time.¹⁵ The marker-MNPs with a hydrodynamic diameter of about 45 nm could prevent the MNPs from being filtered directly into the urine before cleavage and avoid phagocytosis by macrophages, theoretically.¹⁶ We hypothesized that when marker-MNPs are administered to tumor-bearing mice, these marker-MNP probes infiltrate into solid tumor tissues where local overexpressed FAP α cleaves their surface coat of peptides, releasing the reporters that are concentrated into the urine. The reporters have two distinct ligands at the terminus that could be easily detected by ELISA. To validate this hypothesis, in vivo and in vitro studies were performed to assess the tumor-targeting and diagnostic capabilities of the marker-MNPs.

Materials and methods

Peptide nanoparticle synthesis

The N terminus biotinylated and C terminus fluorescent (5-FAM)-labeled reporter peptide (Bio-eGvndneeGffsar-K [5-FAM], lower case = D-isomer; R), reporter control peptide (Bio-eGvndneeGffsar-K [Alexa Fluor 488]; Rc) and marker peptide (Bio-eGvndneeGffsar-K [5-FAM]-GPGPNQC) (Figure S1D and E) were synthesized and characterized by Chinese Peptide Company (Hangzhou, China). The marker peptides were conjugated to aminate Fe₃O₄ MNPs, water-soluble iron oxide nanoparticles with amphiphilic polymer and dextran coating (mean size 30 nm, SHA-30-25; Ocean NanoTech, San Diego, CA, USA), using a disulfide crosslinker, sulfo-LC-SPDP (21,650; Thermo

Fisher Scientific, Waltham, MA, USA), according to the manufacturer's specification. Briefly, sulfo-LC-SPDP and activated MNPs (mole ratio 500:1) in PBS-EDTA (100 mM sodium phosphate, 150 mM NaCl, 1 mM EDTA, 0.02% sodium azide, pH 7.5) were mixed and shaken at room temperature for 30 min. Following purification by magnetic attraction and repeated washes with PBS-EDTA, sulfo-LC-SPDP-derivatized MNPs were made to react in a 1:95:20 (MNPs:peptide:mPEG_{20kDa}-SH) ratio with the sulfhydryl-terminated peptide (the marker peptide is terminated with a cysteine) and mPEG_{20kDa}-SH (Laysan Bio., Inc., Arab, AL, USA) at room temperature overnight in the same buffer.¹⁷ The remaining free succinimidyl groups were quenched by the addition of cysteine (Sigma-Aldrich Co., St Louis, MO, USA), and the marker reporter-encoded MNPs (marker-MNPs) were washed again with PBS-EDTA and stored at 4°C.

The number of 5-FAM-labeled peptides per MNP was determined by absorbance spectroscopy using the absorbance of 5-FAM (492 nm) and its extinction coefficient (78,000/cm/M) or by ELISA (described below). Fluorescence spectra of marker-MNPs and MNPs mixed with an equivalent amount of free marker peptides were measured by microplate fluorescence reader (Ex/Em: 492 nm/500–700 nm). The average relative fluorescence unit was detected by fluorescence microplate reader (Ex/Em: 492 nm/518 nm, Flex Station 3; Molecular Devices LLC, Sunnyvale, CA, USA) for the indicated time. Mean hydrodynamic size of marker-MNPs was analyzed by dynamic light scattering (Nanosight NS300, NanoSight Ltd, Malvern, UK).

Cell lines

The human esophageal squamous cell carcinoma (ESCC) cell line Eca109, human pancreatic cancer cell line PC3 and mouse embryo fibroblast cell line NIH 3T3 were obtained from Cell bank of Chinese Academy of Sciences (Shanghai, China). NIH 3T3 cells transfected with FAP α gene (3T3/FAP α) was constructed in our laboratory. Cells were grown in RPMI 1640 (Thermo Fisher Scientific) supplemented with 10% fetal bovine serum at 37°C and 5% CO₂.

Western blot analysis

Total proteins of cells were separated by 10% sodium dodecyl sulfate-polyacrylamide gel electrophoresis and transferred to polyvinylidene difluoride membranes. After being blocked with 5% non-fat dry milk in PBS, the membrane was incubated with antibodies to FAP α (1:1,000, AF3715; R&D Systems, Inc., Minneapolis, MN, USA), dipeptidyl peptidase 4 (DPP4; 1:1,000, ab28340; Abcam, Cambridge, MA, USA)

or matrix metalloproteinase (MMP)2 (1:1,000, ab86607; Abcam) at 4°C overnight. After being washed several times, the polyvinylidene difluoride membrane was incubated with horseradish peroxidase (HRP)-conjugated secondary antibody at room temperature for 2 hours. The bands were then detected by Pierce ECL Plus Western Blotting Substrate (Thermo Fisher Scientific) according to the manufacturer's protocols. β -Tubulin protein levels were also determined by using the specific antibody (1:3,000, ab126165; Abcam) as a loading control.

Detection of reporter peptides by ELISA

The 96-well plates (Corning Incorporated, Corning, NY, USA) were coated with either 0.8 μ g/mL of anti-FAM antibody (ab19491; Abcam) or anti-Alexa Fluor 488 antibody (Thermo Fisher Scientific) overnight at 4°C. Following wash with PBS and 0.05% (v/v) Tween 20, the plates were blocked with 1% w/v bovine serum albumin (BSA; Sigma-Aldrich Co.) for 2 hours. Urine samples (diluted 1:10–10²) and serial dilution of R or Rc or R in the presence of 10 pM Rc in urine were added and inoculated for 2 hours at room temperature. Following wash, R or Rc captured on the plate was then detected by adding 100 μ L of 0.5 μ g/mL streptavidin-HRP (Thermo Fisher Scientific) for 30 min. After washing, the plates were developed with 50 μ L 3,3',5,5'-Tetramethylbenzidine solution (Thermo Fisher Scientific) for 10 min and quenched with 50 μ L of 1 N HCl before the absorbance of the wells was determined by microplate analysis (SpectraMax Plus; Molecular Devices LLC) at 450 nm.

In vitro stability assays

Marker-MNPs (100 nM by peptide) were incubated in 10% pooled mouse serum (n=6) and 10% pooled urine (n=6) from normal mice at 37°C. At indicated time points, the fluorescence intensity was measured by microplate reader (excitation: 492 nm; emission: 500–700 nm).

In vitro protease assays

Marker-MNPs (10 nM by peptide) were incubated with indicated concentrations of mouse FAP α protein (8647-SE-010; R&D Systems, Inc.) or 1 \times 10⁶ cells of the four cell lines (3T3/FAP α , 3T3, Eca109 and PC3) at 37°C for indicated times. After the marker-MNPs were separated by magnetic attraction, the supernatant was collected and then, for the cleaved reporters, the fluorescence intensity of the supernatant was measured by microplate reader and the concentration was measured by ELISA. Talabostat mesylate (APEXBio Technology, Houston, TX, USA) was used to inhibit FAP α activity.

Reporter peptide renal clearance

Four to six-week-old BALB/c mice were provided by Guangdong Medical Laboratory Animal Center (Guangdong, China). Excretion dose-dependent experiments were performed by intravenous (i.v.) injection of free R or Rc (in 200 μ L of PBS, n=3 mice) followed by collection of all the urine from 0 to 60 min postinjection. Log–log linear fit was performed using average urine concentration from the mice (n=3) at five injected doses. The volume of urine was measured, and the urine was frozen at –80°C until analysis by ELISA. Urinary recovery was calculated as total reporter excreted (the urine reporter concentration multiplied by the urine volume) over total injected dose.

Animal xenograft tumor models and urine collection

Four to six-week-old BALB/c-nude mice were provided by Guangdong Medical Laboratory Animal Center (Guangdong, China) and they were housed under specific pathogen-free conditions in the Laboratory Animal Center of Sun Yat-sen University. All animal experiments were approved by the Experimental Animal Ethics Committee of Sun Yat-sen University and were performed in accordance with the guide for use and care of laboratory animals of the Experimental Animal Committee of Sun Yat-sen University. The mice were inoculated subcutaneously under the right shoulder with 5 \times 10⁶ Eca109 cells. After allowing growth for 4 weeks, the tumor volume reached 100–300 mm³. Then, the tumor-bearing animals (n=10) and the age-matched control mice (n=10) were co-injected via tail vein with marker-MNPs (100 μ L in PBS, 100 or 10 nM by peptide) and Rc (100 or 10 nM). Immediately following infusion, the mice were placed over 12-well plates enclosed by a cylindrical tube to collect all the urine at the indicated time postinjection. Three of them were used to investigate the renal clearance of the marker-MNPs–time curve and 10 of them were subjected to ESCC diagnostic study. One hour postinjection urine was used as the sample for diagnosis of ESCC tumor.

Urine was stored at –80°C directly following collection. Unprocessed urine was diluted 1:10–10² in 1 \times PBS with 1% BSA, and R or Rc in urine was quantified by ELISA (at least two replicates) as described above.

In vivo imaging and biodistribution

In vivo imaging was performed and analyzed at 5–60 min postinjection using a Berthold NightOWL LB 983 Imaging System (Berthold, Bad Wildbad, Germany; excitation=492 nm, emission=518 nm) after the injection of

the marker-MNPs ($n=10$ per group). All images were normalized and analyzed using IndiGo software. For quantitative comparison, regions of interest were drawn over the tumors and muscle, and the average signal ($\times 10^6$ photons/cm²/s) for each area was measured. For the in vivo biodistribution study, mice were sacrificed 1 hour postinjection and the tumor tissues and major organs were carefully harvested. All samples were rinsed with saline, placed on black paper and immediately imaged using IndiGo. For quantitative comparison, regions of interest were calculated as described above.

Immunofluorescence and immunohistochemistry

For immunofluorescence, mice were killed 1 hour postinjection and the tumor tissues were frozen in optimal cutting temperature compound embedding medium and then cut into 4 μ m slices. After blocking with 10% BSA for 30 min, the sections were incubated with rabbit anti-FAP α antibody (1:150; R&D), 4',6-diamidino-2-phenylindole (DAPI) (Thermo Fisher Scientific) and goat anti-FAM (1:200) for 60 min at room temperature in the dark and then visualized with fluorescein isothiocyanate-conjugated donkey anti-rabbit secondary antibody or phycoerythrin-conjugated donkey anti-rabbit and fluorescein isothiocyanate-conjugated donkey anti-goat secondary antibody. Finally, the slices were mounted with DAPI-containing mounting medium under a fluorescence microscope (LSM710; Zeiss).

For immunohistochemistry, formalin-fixed, paraffin-embedded tumor sections were incubated with FAP α antibody (1:100) overnight at 4°C. After washing, an HRP-conjugated secondary antibody was added and the sections were incubated at 37°C for 30 min. The tissue sections were then developed with 3-diaminobenzidine tetrahydrochloride for 10 s, followed by counterstaining with 10% Mayer's hematoxylin.

Statistical analyses

Analysis of variance and Student's *t*-test were performed with GraphPad Prism 5.0 (GraphPad Software, Inc., La Jolla, CA, USA). ELISA data were analyzed using Wilcoxon signed-rank test. The performance of the markers was analyzed by calculating the area under the receiver-operating characteristic (ROC) curve (AUC). $P < 0.05$ was considered statistically significant.

Results

Engineering FAP α -sensitive synthetic biomarkers

The engineered FAP α -sensitive synthetic biomarker was composed of a biotin and 5-FAM-labeled reporter peptide

(Bio-eGvndneeGffsar-K-5-FAM, lower case = D-isomer) and an FAP α -cleavable substrate peptide: GPGPNQC (Figure S1A). The marker peptides (Bio-eGvndneeGffsar-K-(5-FAM)-GPGPNQC) and mPEG_{20kDa}-SH were conjugated to the aminated Fe₃O₄ MNPs via the sulfo-LC-SPDP crosslinker with amine-to-sulfhydryl conjugation by NHS-ester and pyridyldithiol reactive groups (Figure 1A and B). The Fe₃O₄ MNPs were coated with monolayers of oleic acid, amphiphilic polymer and dextran, and they serve as carriers that render it water soluble and provide the free -NH₂. The Fe₃O₄ MNPs were used as they have no toxicity and can be used in vivo. mPEG_{20kDa}-SH was chosen to produce long-circulating MNPs. The substrate peptide has the NQC spacers, two tandem -GP- amino acid bonds and C-terminal cysteine. Two tandem -GP- amino acid bonds are the unique substrate of FAP α , and the C-terminal cysteine allows coupling to MNPs via sulfhydryl group. The reporter peptide is labeled with biotin and fluorescent 5-FAM at the termini and a protease-resistant spacer (Glutamate-Fibrinopeptide B, eGvndneeGffsar), which were selected for their high renal clearance efficiency.⁶ The fluorescence of 5-FAM in the reporter peptide was turned off by intermolecular quenching when closely connected to MNPs and turned on by FAP α cleavage to free the reporter peptides, which were easily detected by the fluorescence (Figure 1C and D). In addition, reporter control peptide (Bio-eGvndneeGffsar-K [Alexa Fluor 488]; Rc) was used to normalize the fluctuation of urine volume and, thus, improved the accuracy of urinary reporter peptide quantification.

The mean size of marker-MNPs was about 45 nm and a surface valence of peptides was about 15–20 peptides per MNP (Figure S1B and C). The marker-MNPs were injected in the blood and they infiltrated the tumor site at which they could be cleaved by FAP α and the reporter peptides could be released; the free reporter peptides passively filtered through the kidney and could be measured in urine by ELISA. The noncleaved marker-MNPs cannot filter directly into the urine because the hydrodynamic diameter of the marker-MNPs is larger than the glomerulus size exclusion limit (~5 nm). The schematic of approach is shown in Figure 2.

The quenching efficiency and stability of marker-MNPs in vitro

Fluorescence spectra of marker-MNPs or MNPs mixed with an equivalent amount of free marker peptides are shown in Figure 1B. The fluorescence intensity of free 5-FAM-labeled marker peptides decreased rapidly (90.8%) after they were conjugated to MNPs. In addition, no fluorescence of marker-MNPs was observed in the in vivo imaging system, whereas

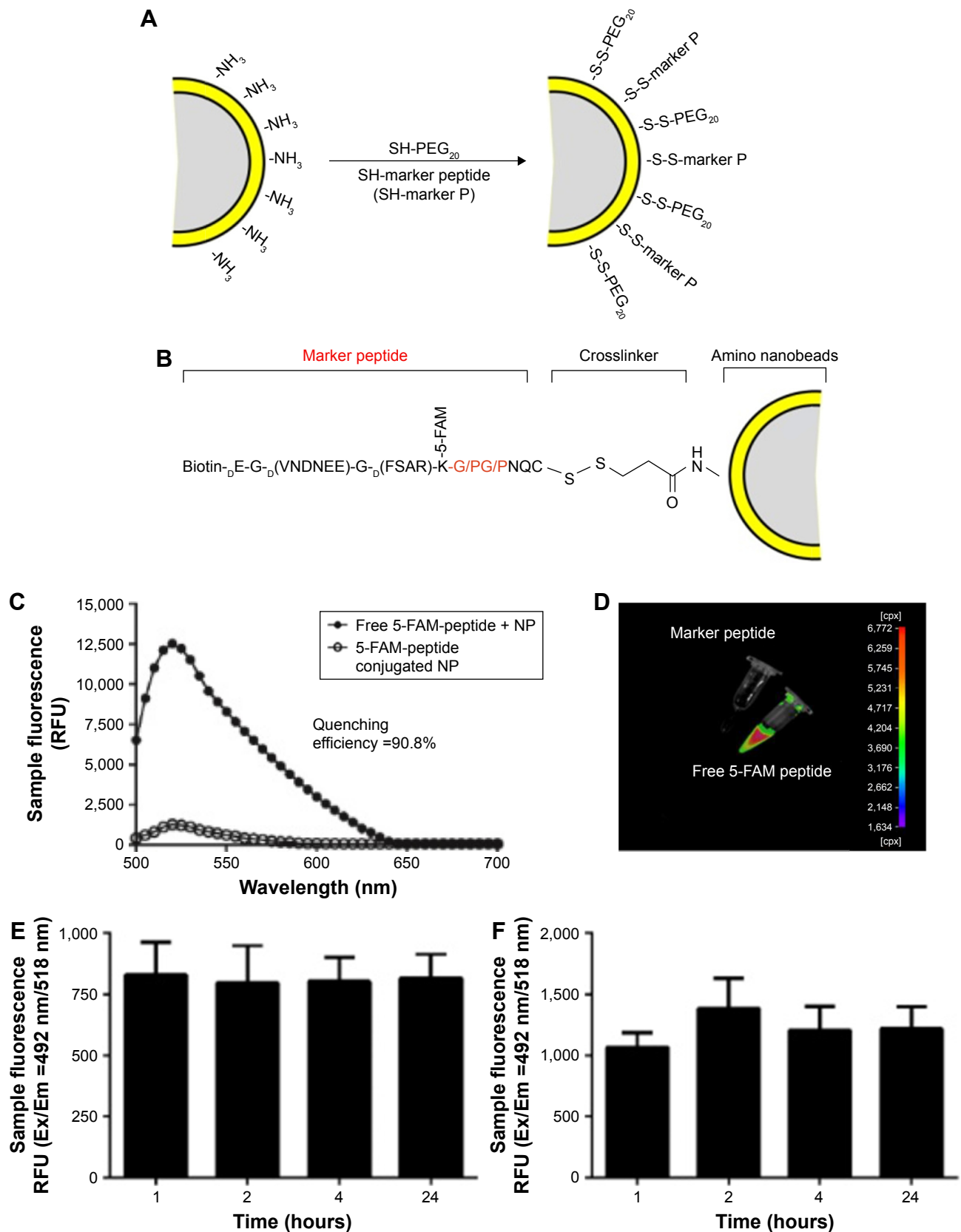


Figure 1 Structure analysis of marker-MNPs.

Notes: (A) Structural diagram of naked nanobeads. (B) Structural diagram of marker-MNPs. Red fonts indicate restriction sites of FAP α . (C) Fluorescence spectra of marker-MNPs conjugated with fluorescein-labeled peptides and naked beads incubated with an equivalent amount of free fluorescein-labeled peptides (excitation: 492 nm; emission: 500–700 nm; quenching efficiency = 90.8%). (D) Fluorescent image of fluorescence quenching. (E) Average fluorescence of marker-MNPs incubated in 10% mouse serum at 37°C over time (excitation: 492 nm; emission: 518 nm). (F) Average fluorescence of marker-MNPs incubated in urine of mice at 37°C over time.

Abbreviations: MNPs, magnetic iron oxide nanoparticles; RFU, relative fluorescence unit.

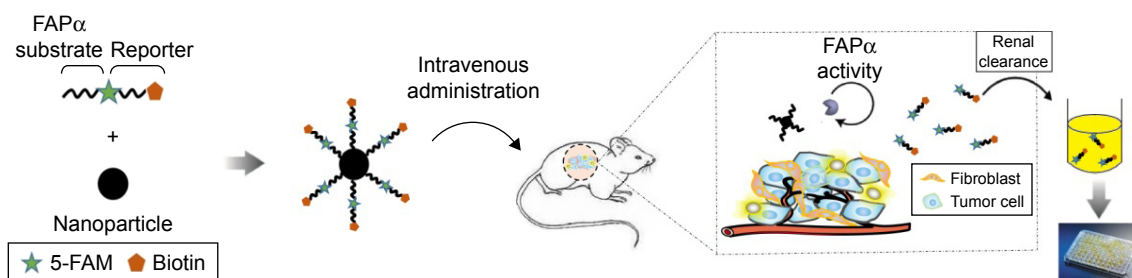


Figure 2 Schematic and design of the approach.

Notes: Marker-MNPs composed of nanobeads conjugated with an FAP α -sensitive substrate in tandem with a ligand-encoded reporter. These agents survey the vasculature for the sites where FAP α cleaves and releases the reporters into urine for analysis by ELISA.

Abbreviations: ELISA, enzyme-linked immunosorbent assay; FAP α , fibroblast activation protein α ; MNPs, magnetic iron oxide nanoparticles.

MNPs mixed with 5-FAM-labeled marker peptides exhibited obvious fluorescence (Figure 1C). The results showed that the marker peptides conjugated with MNPs exhibited high fluorescence quenching efficiency via homoquenching effect.

Furthermore, to test the stability of marker-MNPs in vitro, the marker-MNPs were treated with 10% sera and urine of normal mice, at 37°C overnight. As shown in Figure 1E and F, there was no significant difference of increases in sample fluorescence.

The substrate specificity of marker-MNPs in vitro

A schematic of FAP α -sensitive synthetic biomarker detection is shown in Figure 3A and B. The released 5-FAM-labeled

reporter peptides were captured by anti-FAM antibodies and detected by biotin-streptavidin-HRP, revealing a linear dose dependence from ~100 pM down to the limited detection of 5 pM for reporter peptides in urine (Figure 3C). Similarly, Alexa Fluor 488-labeled reporter control was measured by ELISA and there was no significant interference of Rc to R peptide qualification (Figure 3C and D).

To test the susceptibility and specificity of FAP α -sensitive substrate peptide, marker-MNPs were treated with recombinant FAP α (0.1–100 pM) at 37°C for 1 hour. As shown in Figure 4A, elevated levels of cleaved reporter peptides were detected by ELISA with increasing concentration of FAP α . Moreover, the levels of cleaved reporter peptides were increased over time when treated with 10 nM FAP α , and no

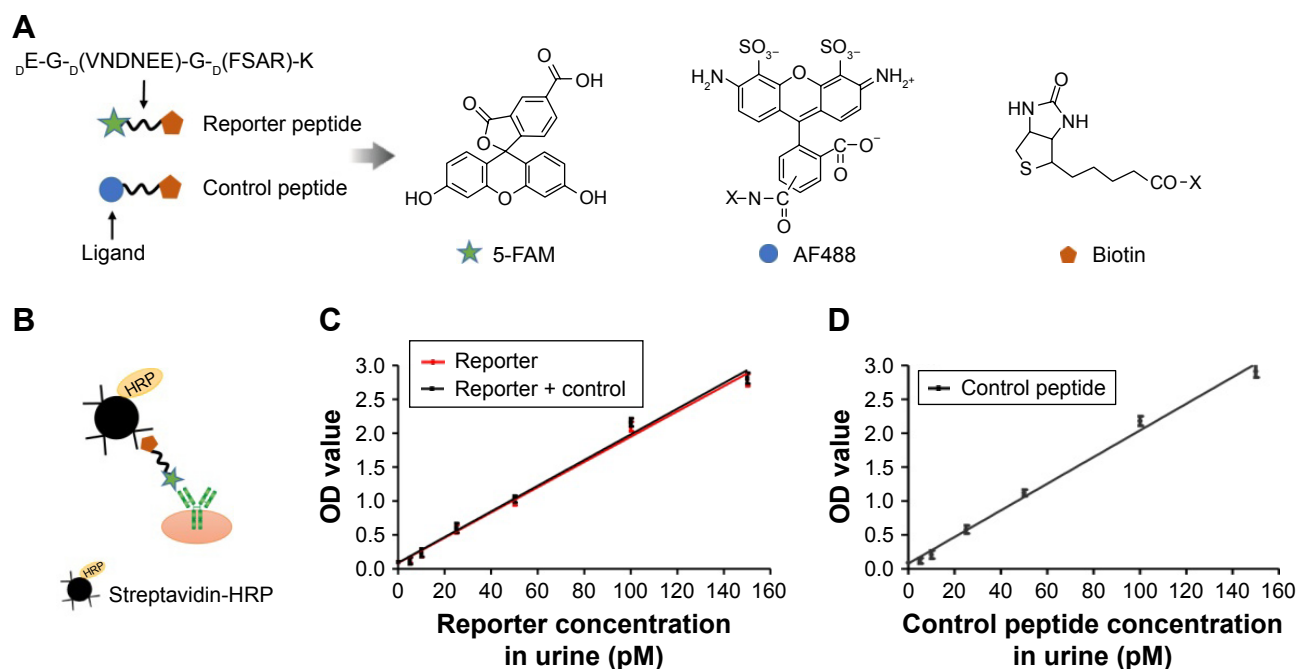


Figure 3 Schematic of urine reporter detection.

Notes: (A) Schematic of ligand-encoded reporter along with chemical structures of associated ligands. (B) Schematic of ELISA sandwich complex. (C) Reporter concentration (R, Rc + R) in urine was detected with anti-FAM antibody by ELISA. (D) Control peptide concentration (Rc) in urine was detected with anti-AF488 antibody by ELISA.

Abbreviations: ELISA, enzyme-linked immunosorbent assay; HRP, horseradish peroxidase; OD, optical density; R, reporter; Rc, reporter control peptide.

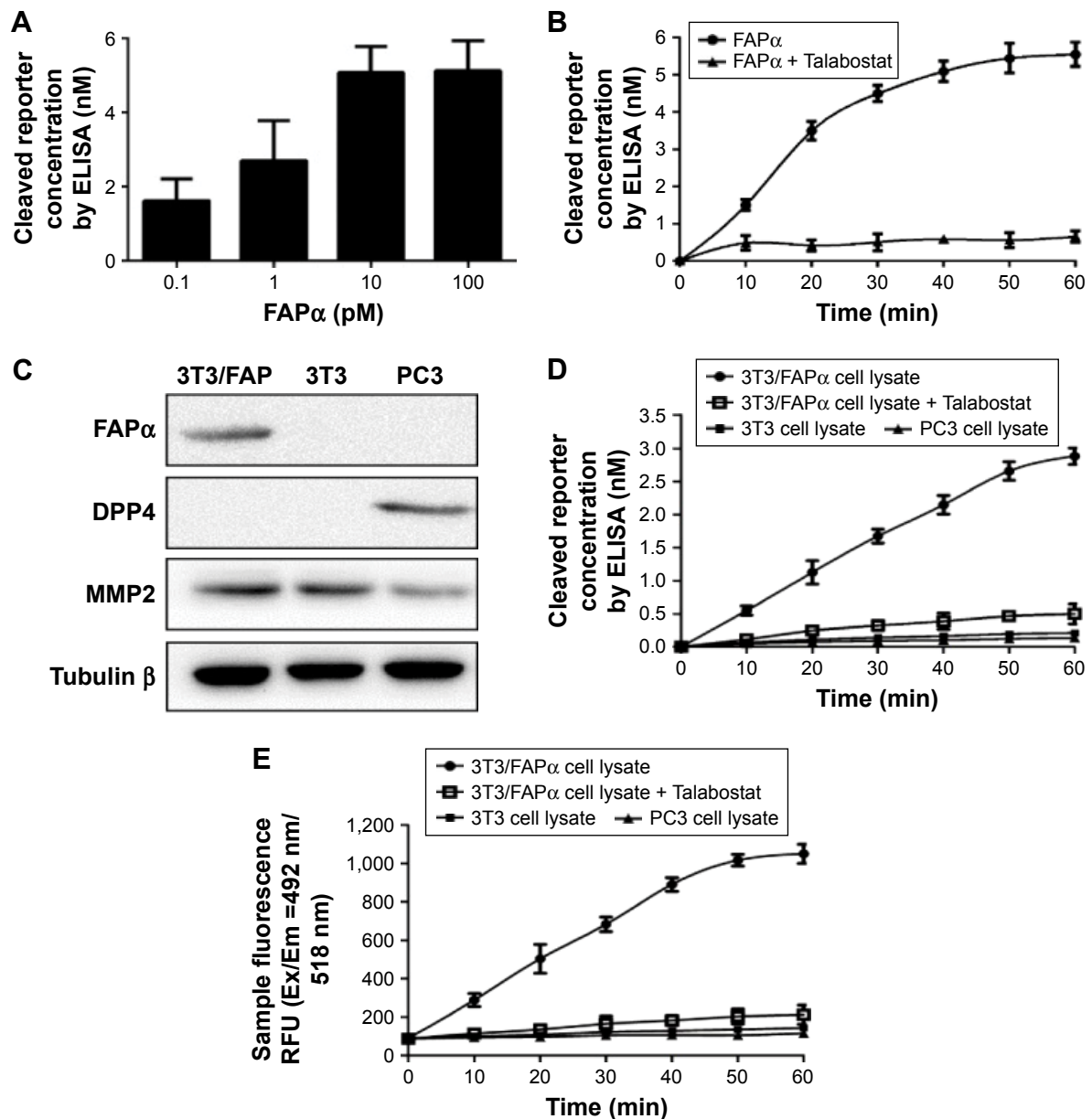


Figure 4 Identification of physicochemical properties of marker-MNPs in vitro.

Notes: (A) Quantification of the level of cleaved reporters released from marker-MNPs after incubation with increasing concentrations of FAP α ($n=3$ per dose, $x \pm SD$). (B) Marker-MNPs incubated with FAP α enzyme (10 nM) or with FAP α enzyme (10 nM) with Talabostat (1 nM). (C) Verification of FAP α , DPP4, MMP2 expression levels in 3T3/FAP, 3T3, PC3 cell lines by Western blotting. (D) Cleaved reporter concentration in the supernatant detected by ELISA after incubation with different cell lysates. (E) Sample fluorescence analysis after incubation with different cell lysates.

Abbreviations: DPP4, Dipeptidyl peptidase-4; ELISA, enzyme-linked immunosorbent assay; FAP α , fibroblast activation protein α ; MMP2, matrix metalloproteinase 2; MNPs, magnetic iron oxide nanoparticles; RFU, relative fluorescence unit.

cleaved reporter peptides were detected when 10 nM FAP α inhibitor Talabostat was added (Figure 4B). Furthermore, 3T3/FAP α cell line, which stably expressed recombinant mouse FAP α (Figure S2A), was used as FAP α -positive cell line (FAP α +). Western blotting showed that FAP α was expressed in 3T3/FAP α cells, and DPP4, a member closely related to FAP α , was expressed in PC3 cells. MMP2 was expressed in all the three cell lines (Figure 4C). Marker-MNPs were incubated with the 3T3/FAP α , 3T3 and PC3

cells, respectively. As shown in Figure 4D, the supernatant of 3T3/FAP α cell line (FAP α +/MMP2+) exhibited increasing fluorescence over time, and fluorescence decreased sharply on treatment with 10 nM Talabostat. Moreover, PC3 cell line (DPP4+/MMP2+) and 3T3 cell line (MMP2+) showed no obvious change in fluorescence within 60 min. The cleaved reporter peptide concentration was also investigated by ELISA and was consistent with the fluorescence result (Figure 4E). These results showed that FAP α can cleave and

release the reporter peptides from marker-MNPs, but DPP4 and MMP2 cannot, suggesting that marker-MNPs have good substrate specificity for FAP α enzyme.

Reporter peptides renal clearance

To investigate the renal clearance efficiency of reporter peptides *in vivo*, free reporter peptides and control peptides were injected into healthy mice via tail vein and urine was collected at 60 min postinjection. A linear relationship between the injection dose and urine concentration was obtained (Figure S2B). In addition, the urinary reporter recovery (total excretion over total reporter injected) did not decrease over 1–200 nM of input dose (Figure S2B). These data showed that the free reporter peptides administered *i.v.* are cleared into urine rapidly and their concentration in urine is directly proportion to the input dose.

In vivo diagnosis of solid tumor by marker-MNPs

It was found in our previous study that the CAFs in ESCC Eca109 xenograft tumor mice expressed high levels of FAP α ¹⁸ and it was further confirmed that activated fibroblasts had very limited capacity to secrete soluble FAP α in blood.¹⁹ So, the Eca109 tumor mice model was used to investigate marker-MNPs for *in vivo* diagnosis of tumors. A dose of 100 nM marker-MNPs was injected into ESCC and healthy mice via tail vein. As shown in Figure S3, the concentration of the cleaved reporter peptide in treated mice urine increased rapidly from 30 min and reached a peak at 60 min and dropped to the bottom line at 150 min postinjection, whereas in the healthy mice, urine reporter was not detectable at 0–180 min and then slightly decreased at 180–300 min. So, 1-hour postinjection urine was selected as the sample for tumor diagnosis.

As the urine reporter concentration was affected by host and environmental factors (eg, diet, drinking, activity level), we used the reporter control to normalize our test based on that co-administered, a free reporter control, which would pass into the urine independent of disease state and could be used to normalize the levels of reporter peptides released by FAP α . To detect tumors, two doses of marker-MNPs were co-injected with the reporter control into ESCC and healthy mice. The concentration of cleaved reporters in the urine of ESCC mice was significantly higher than in healthy mice at 1 hour after injection, as shown in Figure 5A and E ($n=10$ per group; $P<0.0001$), while there was no significant difference in the urine concentration of reporter control between the two groups (Figure 5B and F). The ratio

of the reporter to the reporter control in ESCC mice was also significantly higher than in healthy control mice ($P<0.0001$; Figure 5C and G). Moreover, the ROC curve was plotted to distinguish ESCC from healthy mice, and the AUC was 1.0 with a sensitivity of 100% and a specificity of 100% for the 100 nM group. The AUC was 0.97 (95% CI: 0.94–1.0) with a sensitivity of 90% and a specificity of 97% for the 10 nM group (Figure 5D and H).

Simultaneously, the mice were imaged using the *in vivo* imaging system at selected time points. As shown in Figure 6A, the mice injected with marker-MNPs 1 hour postinjection demonstrated strong fluorescent activation in the tumor region and bladder, compared with control. Then, the mice were sacrificed and the tumor tissues and major organs carefully harvested. Figure 6B and C show that the fluorescence mainly concentrated in the bladder and tumor tissues, compared with the control group. Kidney of tumor-bearing mice gathered more fluorescent substance. Subsequently, immunohistochemistry and immunofluorescence identified that FAP α was highly expressed in the tumor stroma of Eca109 xenograft tumor mice (Figure 6D). These results confirmed that marker-MNPs could be cleaved by FAP α in tumor stroma and the reporter peptide could be released in urine.

Discussion

In this study, we revealed the potential of newly synthesized FAP α -sensitive marker-MNPs in cancer diagnosis. Rather than searching for endogenous biomarkers, the synthetic biomarkers were administered to specifically detect the presence of diseased tissues, just as in the clinical use of positron emission tomography to find the location of metabolically active tumors by a radiolabeled glucose probe. In ESCC mice model, we firstly used FAP α -sensitive marker-MNPs and developed a simple ELISA to detect urinary synthetic biomarkers for solid tumor diagnosis.

Proteases are ideal effector biomolecules in drug delivery when utilized to release cargo at particular locations in the cell compartments. Many proteases that are overexpressed in tumors and tumor-associated cells have been explored to be the enzyme-activated prodrugs or *in vivo* diagnostic probes. Among them, MMPs and cysteine cathepsins (CATs) have commonly been used.^{20,21} However, most of the proteases are also found in high concentration in the serum of patients with tumors. For example, a number of studies reported higher circulating levels and enzyme activities of MMPs (2, 7 or 9) and CATs (B, L and K) in various tumors,^{22–24} suggesting the prodrugs or probes have the potential risk of degradation by these proteases in human blood.

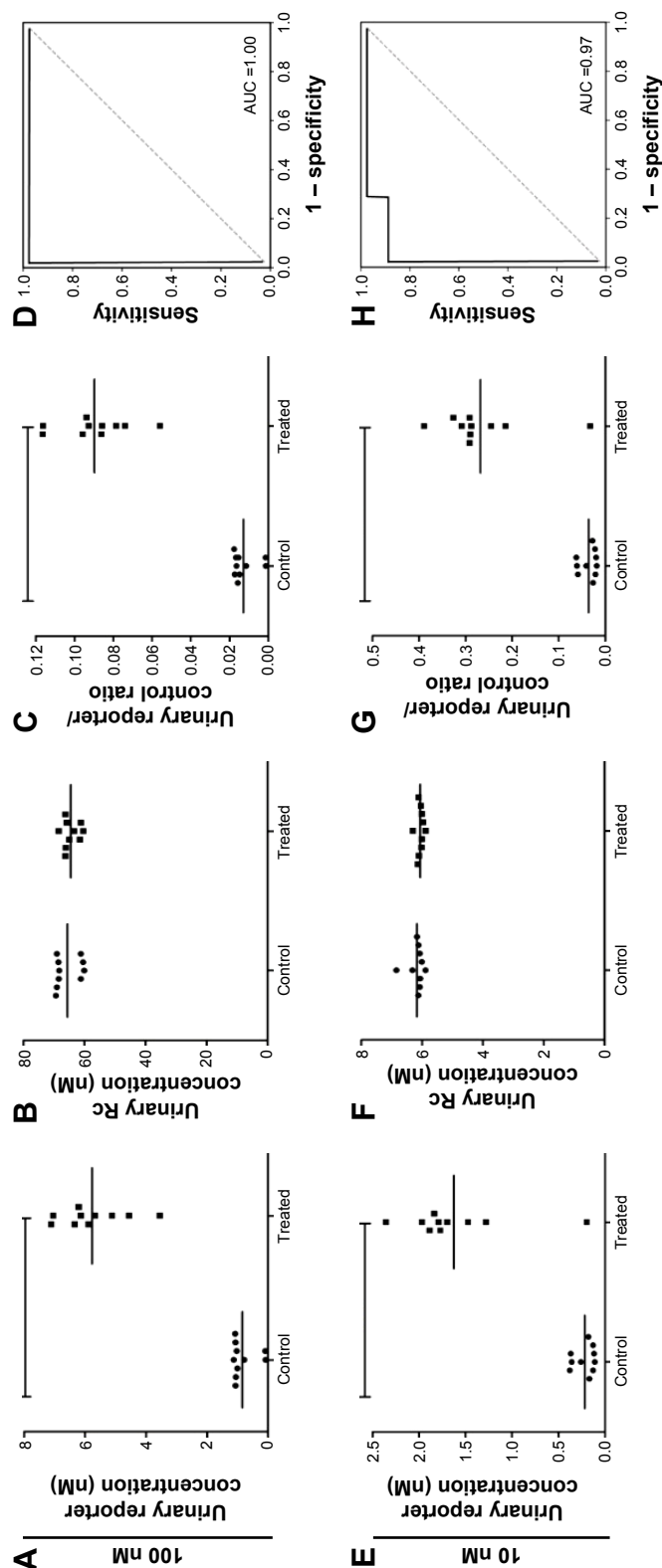


Figure 5 Urinary diagnosis of solid tumor by marker-MNPs.
Notes: Two doses, that is, (A–C) 100 nM and (E–G) 10 nM of marker-MNPs were co-injected with the reporter control into Eca109 tumor-bearing mice and healthy control mice and urinary reporters (R or Rc) were measured by ELISA. (D, H) ROC curve was plotted to distinguish ESCC tumor mice from healthy mice.
Abbreviations: ROC, receiver-operating characteristic; ELISA, enzyme-linked immunosorbent assay; ESCC, esophageal squamous cell carcinoma; MNPs, magnetic iron oxide nanoparticles.

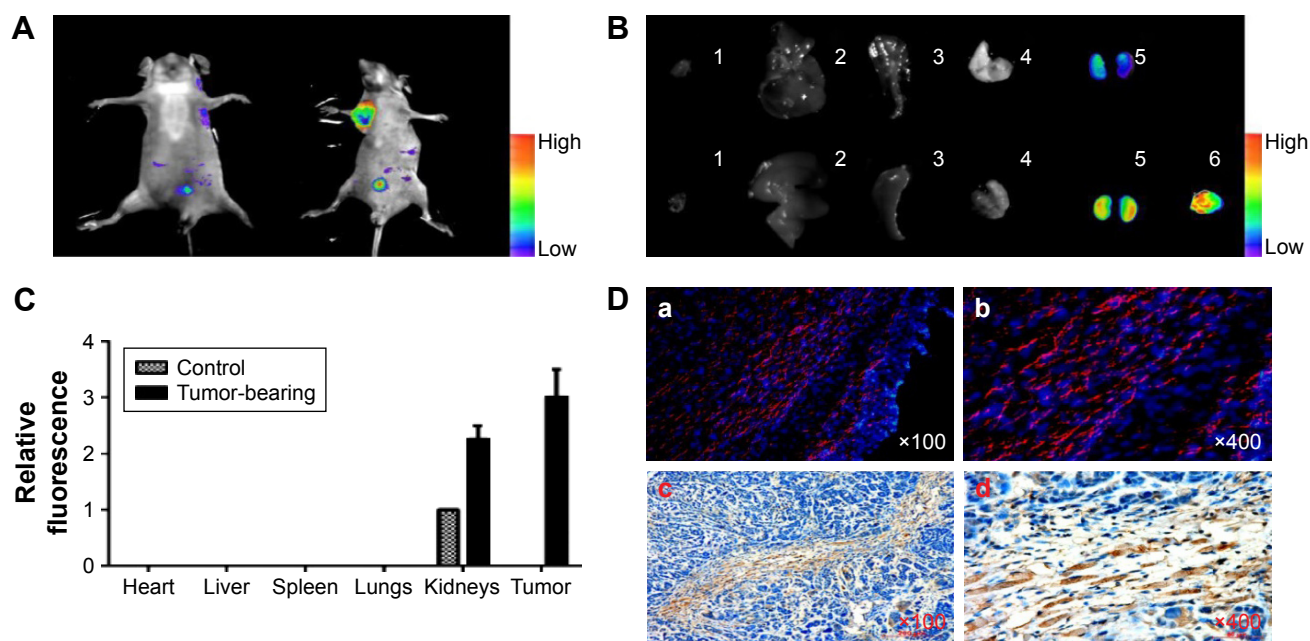


Figure 6 Detection of FAP α enzyme in vivo. Marker-MNPs (100 μ L in PBS, 100 nM by peptide) were injected into Eca109 tumor-bearing mice (treated group) or healthy mice (control group) via tail vein.

Notes: (A) In vivo fluorescence images of healthy mice and Eca109 tumor-bearing mice injected i.v. with marker-MNPs. Images were acquired at 1 hour after injection and were normalized by the maximum average value. The color bar indicates radiant efficiency (low, 0; high, 0.15×10^5). (B) Representative images of dissected organs and tissues of healthy mice (upper row) and Eca109 tumor-bearing mice (lower row) sacrificed at 6 hours after injected i.v. with marker-MNPs. The color bar indicates radiant efficiency (low, 0; high, 0.13×10^5). (C) Relative quantification of the fluorescent signal of organs after the mice were infused with mixtures of marker-MNPs (Student's t-test; $n=8$ mice, SD). (D) Immunofluorescence images of tumor sections injected with marker-MNPs (red; a, b). Tumor sections were counterstained with DAPI (blue; c, d). Analysis of expression of FAP α in Eca109 tumor section by immunohistochemistry.

Abbreviations: DAPI, 4',6-diamidino-2-phenylindole; FAP α , fibroblast activation protein α ; i.v., intravenously; MNPs, magnetic iron oxide nanoparticles.

Recently, accumulated evidence has shown that there is an increasing interest in FAP α -activated drugs and probes, which have been explored in the diagnosis and treatment of various solid tumors.^{25–27} The FAP α -sensitive probe is easily accessible to the tumor due to the special expression of FAP α in CAFs around the tumor cells.²⁸ Interestingly, FAP α showed overexpression in the tumor tissues, but very low levels in the blood of patients.²⁹ In our study, marker-MNPs incubated with serum from mice exhibited good stability in the blood, suggesting FAP α was a valuable target for activatable probes. Also, although DPP4 cleaves the same prolyl peptide (Pro-Xaa) bonds, it is difficult for DPP4 to cleave marker-MNPs due to the space of NQC three peptides which are connected at the end of the prolyl peptide bond. Our study showed that marker-MNPs cannot be cleaved when incubated with DPP4+ or MMP2+ cell lines, suggesting the specificity of proteolytic activity of FAP α for marker-MNPs.

It is important that free reporter peptides are efficient and pass into urine fast. A protease-resistant peptide (Glutamate-Fibrinopeptide B) that served as the reporter space was selected due to its high renal clearance efficiency,⁶ and in this study, its high efficiency of renal clearance and linear dose dependence of excretion were confirmed. The reporter

peptides in urine detected by ELISA were easy to perform and had high sensitivity and specificity.

In view of the urine reporter concentration being affected by host and environment factors, marker-MNPs were co-administered with the reporter control to normalize the levels of reporter peptides released by FAP α , which thus eliminates these interference factors. In line with our previous studies, although Eca109 cells do not express FAP α , the CAFs in Eca109 xenograft tumor mice express high levels of FAP α ;¹⁸ both high and low doses of marker-MNPs were administered to Eca109 xenograft tumor mice and the reporter in urine served as a biomarker with a high diagnostic accuracy (AUC 1.0 and 0.97, respectively) for ESCC. The detection of urinary reporters is better than biomarkers in blood as the complex composition in blood often affects biomarker quantification. Moreover, small inert analytes in plasma, such as our ligand-encoded reporters, were concentrated in the urine. In our animal models, the reporters were enriched to levels that required the urine samples to be diluted (10- to 10^2 -fold) to prevent signal saturation when marker-MNPs were administered at a dose typical of nanomedicines (~ 1 mg/kg).^{30,31} Imaging analysis in vivo also confirmed that cleaved reporters were concentrated in the bladder of tumor-bearing mice.

Limitations

Our study, however, still had some limitations. First, although FAP α -sensitive synthetic biomarkers have the potential to improve disease diagnosis and monitoring, administering synthetic compounds requires rigorous evaluation before use in humans. Urinary synthetic biomarker measured by a higher sensitivity method such as single molecule array technology would use minute doses of marker-MNPs to increase the safety in humans.³² Secondly, further studies are needed to determine how to scale between the mouse and human injecting dose.

Conclusion

In summary, we designed an FAP α -sensitive synthetic biomarker based on the specific endonuclease activity of FAP α in CAF cells. The marker-MNPs were injected into ESCC tumor mice and they reached the tumor tissues where they were cleaved effectively by FAP α to release the reporter peptide and filter it into the urine. Detection of the cleaved marker peptide by ELISA in urine is of low cost, noninvasive and has a high diagnostic accuracy for ESCC. Our results showed that the coating of a fusion peptide containing specific enzyme site on MNPs might be useful for the diagnosis of solid tumors, except for in renal cancer.

Acknowledgments

This work was supported by the National Natural Science Foundation of China (No 81372573, No 81072670). The authors wish to acknowledge Professor Du Jun for helping in the experimental design.

Author contributions

XF, QW, GZ and WL contributed to the conception and design of the study, data acquisition, data analysis and manuscript writing. YW, YL and XZ contributed to data analysis and manuscript writing. All authors contributed toward data analysis, drafting and revising the paper and agree to be accountable for all aspects of the work.

Disclosure

The authors report no conflicts of interest in this work.

References

- Schroeder A, Heller DA, Winslow MM, et al. Treating metastatic cancer with nanotechnology. *Nat Rev Cancer*. 2011;12(1):39–50.
- Lee S, George Thomas R, Ju Moon M, et al. Near-infrared heptamethine cyanine based iron oxide nanoparticles for tumor targeted multimodal imaging and photothermal therapy. *Sci Rep*. 2017;7(1):2108.
- Dudani JS, Jain PK, Kwong GA, Stevens KR, Bhatia SN. Photoactivated spatiotemporally-responsive nanosensors of in vivo protease activity. *ACS Nano*. 2015;9(12):11708–11717.
- Warren AD, Gaylord ST, Ngan KC, et al. Disease detection by ultra-sensitive quantification of microdosed synthetic urinary biomarkers. *J Am Chem Soc*. 2014;136(39):13709–13714.
- Kwong GA, von Maltzahn G, Murugappan G, et al. Mass-encoded synthetic biomarkers for multiplexed urinary monitoring of disease. *Nat Biotechnol*. 2013;31(1):63–70.
- Lin KY, Kwong GA, Warren AD, Wood DK, Bhatia SN. Nanoparticles that sense thrombin activity as synthetic urinary biomarkers of thrombosis. *ACS Nano*. 2013;7(10):9001–9009.
- Gajewski TF, Schreiber H, Fu YX. Innate and adaptive immune cells in the tumor microenvironment. *Nat Immunol*. 2013;14(10):1014–1022.
- Koczorowska MM, Tholen S, Bucher F, et al. Fibroblast activation protein- α , a stromal cell surface protease, shapes key features of cancer associated fibroblasts through proteome and degradome alterations. *Mol Oncol*. 2016;10(1):40–58.
- Liu F, Qi L, Liu B, et al. Fibroblast activation protein overexpression and clinical implications in solid tumors: a meta-analysis. *PLoS One*. 2015;10(3):e0116683.
- Wild N, Andres H, Rollinger W, et al. A combination of serum markers for the early detection of colorectal cancer. *Clin Cancer Res*. 2010;16(24):6111–6121.
- Werner S, Krause F, Rolny V, et al. Evaluation of a 5-marker blood test for colorectal cancer early detection in a colorectal cancer screening setting. *Clin Cancer Res*. 2016;22(7):1725–1733.
- Javidroozi M, Zucker S, Chen WT. Plasma seprase and DPP4 levels as markers of disease and prognosis in cancer. *Dis Markers*. 2012;32(5):309–320.
- Baird SK, Rigopoulos A, Cao D, et al. Integral membrane protease fibroblast activation protein sensitizes fibrosarcoma to chemotherapy and alters cell death mechanisms. *Apoptosis*. 2015;20(11):1483–1498.
- Ruger R, Tansi FL, Rabenhold M, et al. In vivo near-infrared fluorescence imaging of FAP-expressing tumors with activatable FAP-targeted, single-chain Fv-immunoliposomes. *J Control Release*. 2014;186:1–10.
- Xu Q, Ensign LM, Boylan NJ, et al. Impact of Surface Polyethylene Glycol (PEG) density on biodegradable nanoparticle transport in mucus ex vivo and distribution in vivo. *ACS Nano*. 2015;9(9):9217–9227.
- Rosen JE, Chan L, Shieh DB, Gu FX. Iron oxide nanoparticles for targeted cancer imaging and diagnostics. *Nanomedicine*. 2012;8(3):275–290.
- Park JH, von Maltzahn G, Zhang L, et al. Systematic surface engineering of magnetic nanoworms for in vivo tumor targeting. *Small*. 2009;5(6):694–700.
- Liao Y, Xue Y, Zhang L, Feng X, Liu W, Zhang G. Higher heat shock factor 1 expression in tumor stroma predicts poor prognosis in esophageal squamous cell carcinoma patients. *J Transl Med*. 2015;13:338.
- Liao Y, Xing S, Xu B, Liu W, Zhang G. Evaluation of the circulating level of fibroblast activation protein α for diagnosis of esophageal squamous cell carcinoma. *Oncotarget*. 2017;8(18):30050–30062.
- Qifan W, Fen N, Ying X, Xinwei F, Jun D, Ge Z. iRGD-targeted delivery of a pro-apoptotic peptide activated by cathepsin B inhibits tumor growth and metastasis in mice. *Tumour Biol*. 2016;37(8):10643–10652.
- Liu Y, Feng J, Shi L, et al. In situ mechanical analysis of cardiomyocytes at nano scales. *Nanoscale*. 2012;4(1):99–102.
- Klupp F, Neumann L, Kahlert C, et al. Serum MMP7, MMP10 and MMP12 level as negative prognostic markers in colon cancer patients. *BMC Cancer*. 2016;16:494.
- Gong L, Wu D, Zou J, et al. Prognostic impact of serum and tissue MMP-9 in non-small cell lung cancer: a systematic review and meta-analysis. *Oncotarget*. 2016;7(14):18458–18468.
- Liu WL, Liu D, Cheng K, et al. Evaluating the diagnostic and prognostic value of circulating cathepsin S in gastric cancer. *Oncotarget*. 2016;7(19):28124–28138.
- Li J, Chen K, Liu H, et al. Activatable near-infrared fluorescent probe for in vivo imaging of fibroblast activation protein- α . *Bioconjug Chem*. 2012;23(8):1704–1711.

26. Keane FM, Yao TW, Seelk S, et al. Quantitation of fibroblast activation protein (FAP)-specific protease activity in mouse, baboon and human fluids and organs. *FEBS Open Bio*. 2013;4:43–54.
27. Tansi FL, Ruger R, Bohm C, et al. Potential of activatable FAP-targeting immunoliposomes in intraoperative imaging of spontaneous metastases. *Biomaterials*. 2016;88:70–82.
28. Yi X, Wang F, Qin W, Yang X, Yuan J. Near-infrared fluorescent probes in cancer imaging and therapy: an emerging field. *Int J Nanomedicine*. 2014;9:1347–1365.
29. Milner JM, Kevorkian L, Young DA, et al. Fibroblast activation protein alpha is expressed by chondrocytes following a pro-inflammatory stimulus and is elevated in osteoarthritis. *Arthritis Res Ther*. 2006; 8(1):R23.
30. Che L, Zhou J, Li S, et al. Assembled nanomedicines as efficient and safe therapeutics for articular inflammation. *Int J Pharm*. 2012;439(1–2): 307–316.
31. Uchegbu IF, Siew A. Nanomedicines and nanodiagnostics come of age. *J Pharm Sci*. 2013;102(2):305–310.
32. Schubert SM, Arendt LM, Zhou W, et al. Ultra-sensitive protein detection via Single Molecule Arrays towards early stage cancer monitoring. *Sci Rep*. 2015;5:11034.

Supplementary materials

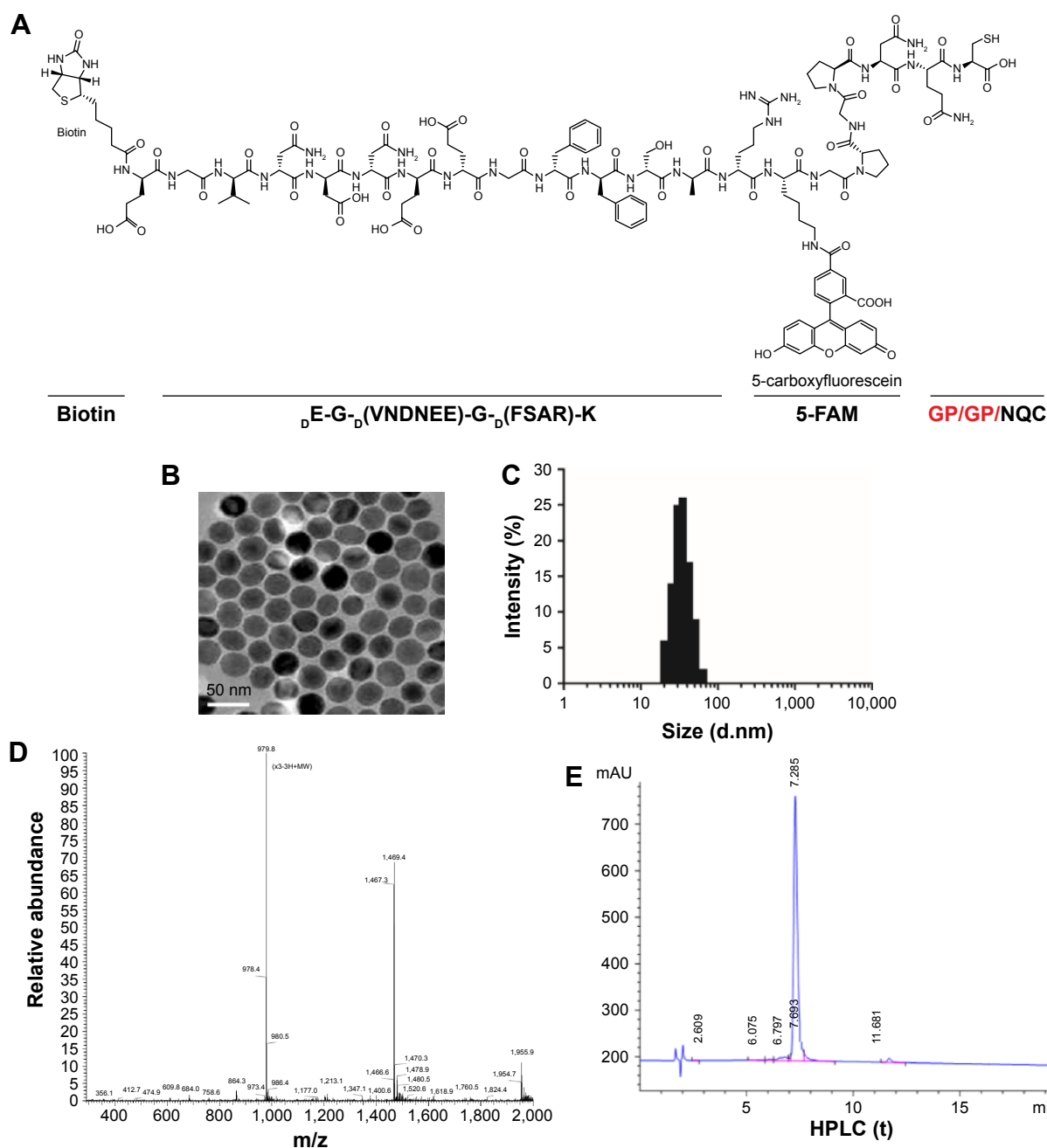


Figure S1 Structures and characterization of peptide-conjugated synthetic nanoprobe.

Notes: (A) Structures of peptide-conjugated synthetic nanoprobe. Red fonts indicate restriction sites of FAP α . (B) TEM images of the magnetic iron oxide beads (MNPs). (C) Size distribution of the MNPs after conjugation. (D, E) MS and HPLC identification of synthetic substrate peptide of FAP α .

Abbreviations: FAP α , fibroblast activation protein α ; HPLC, high-performance liquid chromatography; MNPs, magnetic iron oxide nanoparticles; MS, mass spectroscopy; TEM, transmission electron microscopy.

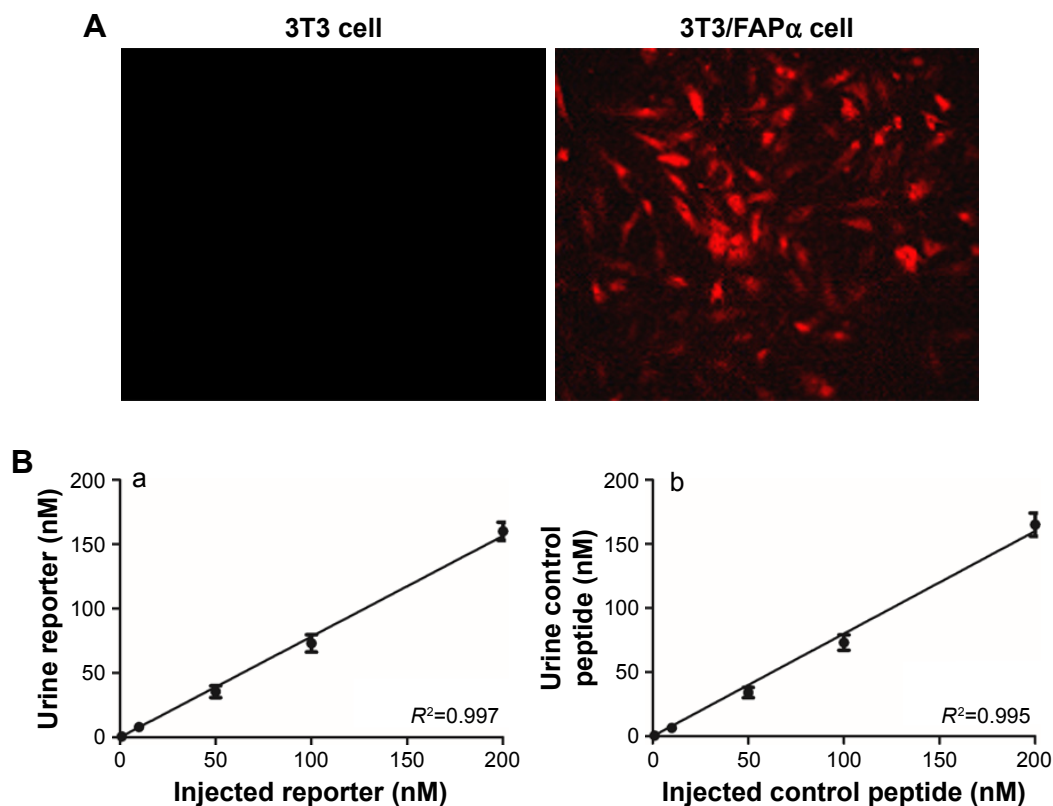


Figure S2 Identification of 3T3/FAP α cell line and renal clearance of reporter peptides.

Notes: (A) Photo of 3T3 cell (left) and 3T3/FAP α cell successfully transferred fluorescence plasmid expressing FAP α and TdTomato fluorescent protein (right). (B) Renal clearance of reporter peptide and reporter peptide control. Serial dilutions of reporter peptide (a) and control peptide (b) were injected into healthy mice via tail vein. Concentration of reporter peptide or control peptide in urine was detected by ELISA. Magnification $\times 200$.

Abbreviations: ELISA, enzyme-linked immunosorbent assay; FAP α , fibroblast activation protein α .

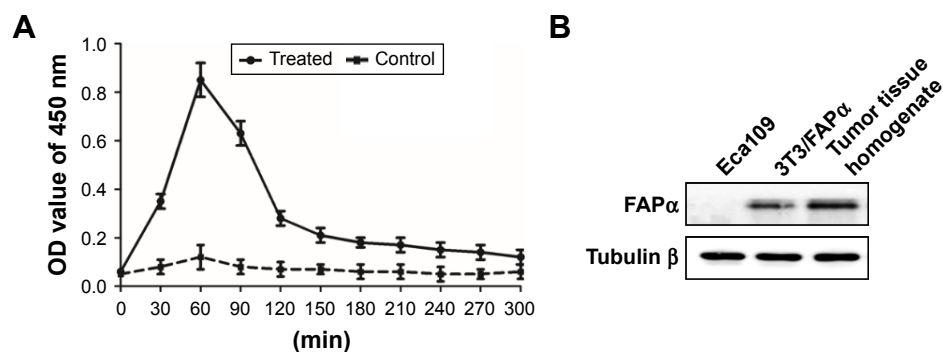


Figure S3 Elisa and Western blot results of detection of FAP α enzyme in vivo.

Notes: (A) Synthetic nanoprobe (100 μ L in PBS, 100 nM by peptide) was injected into Eca109 tumor-bearing mice (treated group) or healthy mice (control group) via tail vein. Figure shows changes in reporters' concentration in the urine of two groups of animals within 300 min. (B) Western blotting analysis of FAP α expression in Eca109 cells, 3T3/FAP α cells and tumor tissue homogenate from xenograft tumor mice models.

Abbreviation: FAP α , fibroblast activation protein α .

International Journal of Nanomedicine

Publish your work in this journal

The International Journal of Nanomedicine is an international, peer-reviewed journal focusing on the application of nanotechnology in diagnostics, therapeutics, and drug delivery systems throughout the biomedical field. This journal is indexed on PubMed Central, MedLine, CAS, SciSearch®, Current Contents®/Clinical Medicine,

Submit your manuscript here: <http://www.dovepress.com/international-journal-of-nanomedicine-journal>

Dovepress

Journal Citation Reports/Science Edition, EMBASE, Scopus and the Elsevier Bibliographic databases. The manuscript management system is completely online and includes a very quick and fair peer-review system, which is all easy to use. Visit <http://www.dovepress.com/testimonials.php> to read real quotes from published authors.